Study on laser welding of AISI 316L austenitic stainless steel

O. DONTU[a], J. L. OCAÑA MORENO[b], R. CIOBANU[a], M. BRANZEI[c*], D. BESNEA[a]
[a]*University "Politehnica" of Bucharest, Department of Mechatronics and Precision Mechanics, 313 Splaiul Independentei, Sector 6, 060042 Bucharest,Romania*
[b]*Centro Laser- UPM, Edificio Tecnológico "La Arboleda", Madrid, Postal Code: 028031, Spain;*
[c]*University "Politehnica" of Bucharest, Metallic Material Science, Physical Metallurgy Depart*ment*, 313 Splaiul Independentei, Sector 6, 060042 Bucharest,Romania*

In this paper is presented a complex analysis for laser welding of AISI 316L austenitic stainless steel in case of three different laser sources: Nd:YAG - λ=1060nm, Laser Diode - λ=904 nm and CO_2 laser - λ=10.6 μm. The laser power input has a specific nonlinear influence on the absorptivity of material for each laser radiation wavelength. In case of CO_2 laser unit, for the welding parameters selected (laser spot diameter-3mm, speed-10mm/s), by increasing the power from 2kW to 2.5kW, the weld bead geometry undergoes minimal changes, meaning energy losses. In contrast, in case of Laser Diode unit, the weld bead geometry undergoes significant changes for the same input parameters. Increasing the initial temperature of the base material around 140°C leads to a partial disappearance of the plastic deformation tensions in the material (shear bends), without affecting the structure (grain size and roundness).

(Received August 18, 2015; accepted September 9, 2015)

Keywords: Laser welding, Hardness, Bead profile, AISI 316L austenitic stainless steel

1. Introduction

Laser welding is a widespread industrial process as a result of the high degree of automation and, therefore, of the increased production rate, strict control over temperature, reduced heat affected zone and increased ratio of the penetration depth/weld seam width [1]. Given their exceptional mechanical properties, corrosion resistance and weldability, austenitic stainless steels are very heavily used in a wide range of areas: storage tanks and containers for corrosive liquids, blast-pressure tanks, specialized equipment in chemical, pharmaceutical and petrochemical industries [2, 3]. When welding equipments that operates in a corrosive environment, formation of cracks in the fusion zone and heat affected zone of the material is the main disadvantage, because cracks propagate over time and may have catastrophic effects on the mechanisms/structures where they occur and even on environment [4]. In the laser welding of austenitic stainless steels an important issue is the appearance of areas sensitive to the formation of cracks that lead to the intergranular and transgranular corrosion of the weld and heat-affected zone.

Laser welding of austenitic stainless steels involves three subzones: the recrystallized grain growth zone, the grain recrystallization zone and the crystallization-free subzone. Grain size directly influences the degree of sensitivity to cracks formation in the weld zone (it decreases with decreasing grain size), as well as other physical characteristics of the material [5]. Therefore, it directly influences the quality of the weld seam.

This paper presents a comprehensive analysis of the material structure in the weld zone in the case of laser welding of AISI 316L austenitic steel and provides information for choosing the appropriate laser generator type and work parameters when combining components of AISI 316L steel. In practical situations during the welding process a very important issue although often neglected is the influence of the initial temperature of the base material [6], and thus, of the temperature gradient, over the structure of the material in the weld zone as well as its physical properties. Taking this into account, in this paper the influence of the initial temperature of the base material in the case of laser welding of the AISI 316L material has been analyzed [7, 8]. Three types of laser generators were used to perform the welding tests that highlighted the influence of the laser radiation wavelength on the structure of the molten material as well as the degree of absorption in the case of AISI 316L steel[9, 10].

2. Experimental procedure

The laser welding tests were carried out on AISI 316L stainless steel plates with the dimensions 160/80/6mm.

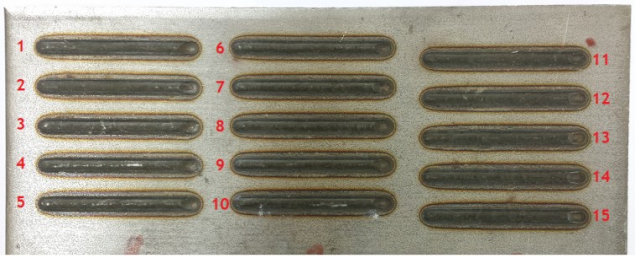

Fig. 1. Experimental sample

For each experimental sample (Fig.1), by keeping constant the input parameters of laser radiation 15 welding seams with different values for the initial temperature of the base material(between 50-140°C) were made.

The chosen laser spot diameter was 3 mm, a condition imposed by the diode laser system, and the chosen speed was 10 mm/s (Table 1).

The power of the laser, the radiation wavelength and the initial temperature of the base material were varied and monitored during experimental tests according to Table 1.

Table 1- Laser welding parameters

P [kW]	Wavelength [nm]	D [mm]	Speed [mm/s]	Number of weld bead	$T_{initial}$ [°C]
1.5	904	3	10	15	50-140
	1060			15	50-140
	10600			15	50-140
2.0	904	3	10	15	50-140
	1060			15	50-140
	10600			15	50-140
2.5	904	3	10	15	50-140
	1060			15	50-140
	10600			15	50-140

Three types of laser units were used for welding: 1. a ROFIN DL 027S laser diode system (λ=904nm), with a maximum radiation power of 2700 W(λ= 904nm), 2. a laser unit with solid active medium Nd:YAG ROFIN DY033(λ=1064 nm), which can develop a maximum power of 3300 W with a yield of 7%, and 3. a CO_2 ROFIN DC035 laser (λ = 10600 nm), with a maximum radiation power of 3500W, coupled to a SEF Roboter, Remote Welding System for positioning the beam in the work area, while providing a generous three-dimensional work space and exceptional positioning accuracy.

The experimental arrangement includes a FLUKE thermocouple linked to the laser head through a protection tube, with the sensing element placed at 20 mm away from the focal point of the laser beam (Fig. 2). In this way, the thermocouple can routinely capture the initial temperature of welding samples for each seam.

Fig. 2-Laser welding system

During the laser welding process helium at a flow rate of 15l/min was used as a shielding gas of the laser head.

Following welding the samples were sectioned across the welding lines, in the middle area, and were subjected to a complex analysis for the characterization of the molten material profile.

Characterisation has been performed using a metallographic microscope OLYMPUS 900, an Image Analysis System (REICHERT UnivaR microscope with Buehler Enterprise Software) and a Hanneman microhardness testing system (Epitip, Carl Zeiss, Jena).

3. Results and discussion

3.1 Wavelength dependence of laser penetration depth in the case of AISI316L steel

Laser beam energy absorption in metals is accomplished via the free electrons in the material, whose coupling with the atoms of the material is however poor. Therefore, only a small amount of the energy captured in the electron cloud is delivered to the atoms of the material and the difference is reemitted outwards as photons of wavelength identical with that of the incident radiation. To summarise, the smaller the wavelength, the higher the probability of producing atomic vibrations instead of electronic ones. Thus, a better coupling of the beam energy with the processed material results [10, 11].

In order to track the influence of the laser radiation wavelength on the profile and characteristics of the material in the heat-affected zone, the three laser units, mentioned in section 2 were used. For the results to be conclusive three different power modes were set: 1.5 kW, 2 kW, 2.5 kW. The operating speed was 10mm/s, the spot diameter - 3mm and the initial temperature of the material was 30°C. For better convenience these details can be also seen in table 2.

For accurate measurements, for each power mode 3 weld seams were made. The penetration depth for each one has been recorded and an average has been calculated.

Table 2. Influence of laser wavelength and power on penetration depth

P [kW]	**LD**	**CO_2**	**Nd:YAG**
	Average penetration depth, [mm]		
1.5	**0.50**	**0.30**	**0.49**
2.0	**1.45**	**0.39**	**0.75**
2.5	**1.72**	**0.45**	**0.85**

In the case of AISI316L austenitic stainless steel the experimental results confirm the studies in the field [10] and the dependence of the penetration depth on power and wavelength is concretely established (Table 2 and Fig. 3).

From Fig. 3 one can notice that the difference between the absorptivity at the 3 wavelengths increases with the laser radiation power. While for the input power of 1.5 kW, the differences between the penetration depth for all three wavelength levels are reduced, for the input

power of 2.5 kW, in case of laser generator with wavelength of 904nm, the absorptivity of the material increases exponentially, reaching a penetration depth two times higher than in the case of the laser unit with a 1060nm wavelength and approximately 5 times higher than in the case of the laser generator with wavelength of 10600nm.

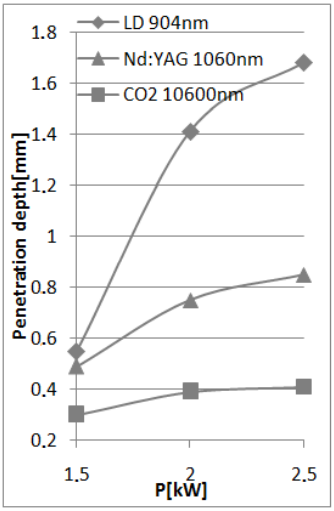

Fig. 3- Influence of laser radiation wavelength on material absorption

In the laser welding process, laser radiation parameters must ensure a temperature growth in the joining area up to a value between the melting and the boiling point of materials [11].

$$T_{melting} < T_{ms} < T_{vaporization} \quad (1)$$

where: T_{ms} is the temperature in the first layer of the material from the laser beam action area.

The duration of the action of the laser or the moving speed of the parts/beam are chosen so that penetration of the melting front in the materials might take place before the beginning of the evaporation of their surface layer. Thus, the maximum depth of the melt is achieved when the surface temperature of the material reaches the boiling point [12].

The expression of the temperature field in welded materials in relation to the intensity of the flux absorbed per area unit-I_0, the radial distance – r from the centre of the laser spot, the depth of penetration into the material – z and time – t may be determined by the relation:

$$T_{(r,z,t)} = \frac{I_0 a^2}{k} \cdot \sqrt{\frac{d}{\pi}} \cdot \int_0^{\tau_i} \frac{e^{-\frac{z^2}{4dt}} e^{-r^2(4dt+a^2)}}{\sqrt{t}(4dt+a^2)} \quad (2)$$

where: τ_i= time length of the laser pulse.

By imposing certain conditions, the C_t thermal time constant can be defined, as the time interval in which the temperature of the deep mass of the molten material is of the same order as the temperature of the laser-irradiated surface. When the duration of action of the laser is much smaller (excessive movement speed) than the thermal time constant T_{tC} of the material to be welded, no homogenous melting of the materials is achieved in the area of the weld seam, which has unfavourable repercussions on the quality of the welded assemblies. In conclusion, for optimal energy efficiency and high quality of juncture in the case of laser welding, the wavelength and power of the laser generator are two parameters that must be perfectly harmonized with the welding speed and the type of material used [12].

In the case of the AISI 316L austenitic stainless steel analyzed in this paper, for the CO_2 laser generator (wavelength 10600nm), the penetration depth for the input power P=2.5kW is almost identical to the depth for P=2kW power, given that a saturation of the coupling of the laser beam photons and material occurs [11]. As a result, in the case of a 2.5 kW power, the absorption rate decreases, a part of the radiation is reflected and another part produces the evaporation of the material from the surface of the material.

3.2 Microstructure analysis

Microstructure analysis was performed using a metallographic microscope OLYMPUS 900, an Image Analysis System (REICHERT UnivaR microscope with Buehler Enterprise Software). In laser welding process special attention must be given to the influence of the initial temperature of the base material on the structural changes that occur in the welding zone [13, 14].

Regarding this aspect, for a initial temperature of the base material between 50°C and 140°C, the maximum depth of penetration in case of the three types of laser generators considered here was monitored (Table 4). A small increase in the maximum penetration depth as well as shape and structural changes in the molten material were obtained depending on the initial temperature of the material. The maximum penetration depth changes because of the internal energy accumulated by the material through preheating, but also because of the changes at molecular level that make the atoms vibrate and allow for a better coupling of the photons in the laser spot.

Considering the multitude of samples achieved in the project and taking into account that most significant changes on laser penetration depth values were registered for Nd:YAG (λ=1060 nm) and Laser Diode (λ=904 nm), the microstructural, geometry and micro-hardness analysis were done only for this two laser units, for which were preserved the same input parameters, i.e. LASER power 2.5 kW and speed 10mm/s.

Microstructure investigations were carried out using the REICHERT UnivaR microscope with Buehler Enterprise analysis system. Depending on the welding parameters, the surface of the resulting seam section varies, as shown in Table 4. It displays a sensitive enlargement of the surface with the variation of the initial temperature of the material, as well as a considerable increase depending on the wavelength of the laser radiation (Fig. 4).

Table 4- Maximum depth of penetration in case of the three types of laser generators

Ti [°C]	Nd:YAG			LD			CO_2		
	Depth, [mm]			Depth, [mm]			Depth, [mm]		
	1.5kW	2kW	2.5kW	1.5kW	2kW	2.5kW	1.5kW	2kW	2.5kW
50	0.56	0.73	0.83	0.52	1.52	1.71	0.31	0.41	0.50
60	0.76	0.69	0.91	0.61	1.65	1.64	0.34	0.45	0.45
70	0.72	0.78	0.75	0.66	1.70	1.66	0.32	0.48	0.54
80	0.65	0.67	1.06	0.66	1.70	1.76	0.34	0.42	0.44
90	0.73	0.78	0.88	0.67	1.66	1.75	0.37	0.48	0.49
95	0.68	0.71	1.05	0.63	1.72	1.66	0.36	0.51	0.47
100	0.71	0.74	0.93	0.66	1.87	1.87	0.35	0.45	0.45
105	0.74	0.83	0.90	0.64	1.75	1.86	0.37	0.52	0.47
110	0.70	0.8	1.02	0.63	1.79	1.89	0.39	0.49	0.47
115	0.64	0.92	0.94	0.68	1.78	1.95	0.37	0.45	0.45
120	0.76	0.8	0.81	0.75	1.80	1.82	0.39	0.51	0.47
125	0.72	0.91	0.98	0.70	1.69	1.93	0.37	0.52	0.48
130	0.65	0.84	0.95	0.71	1.86	2.03	0.38	0.53	0.68
135	0.67	0.88	0.94	0.73	1.86	1.95	0.43	0.53	0.53
140	0.72	0.98	1.02	0.72	1.85	1.94	0.41	0.59	0.53

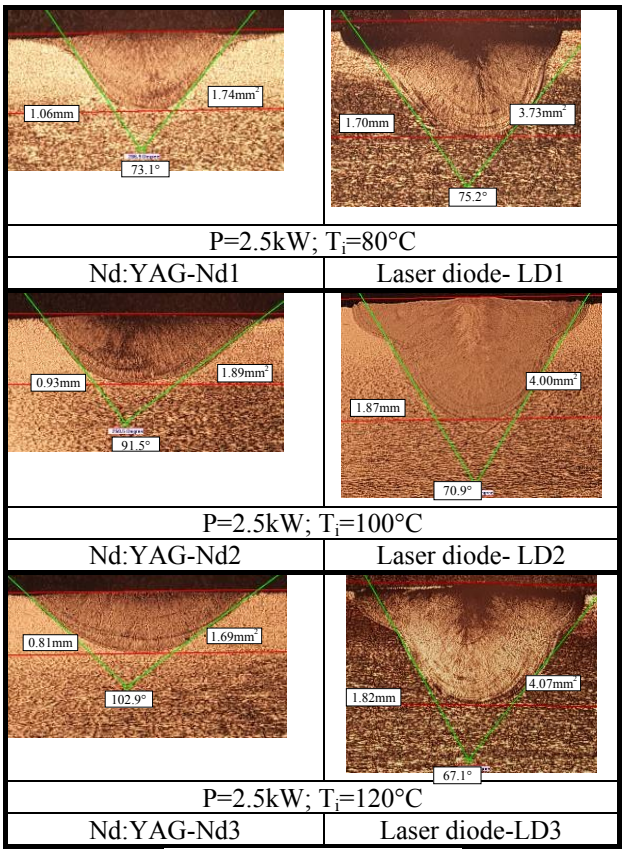

Fig. 4. Welding seams sections

In all sections of the welding seams, a solidification structure with a more or less symmetrical thermal axis is formed, depending on its cooling rate. The structure is a single-phase, columnar, with relatively uniform and fine grains as it results from microstructure characterisation (Fig.5). The depth of the welding seam varies in the same direction, thus confirming the influence of the variation of welding parameters. The thermal-influence zone varies depending on the initial temperature of the base material, being mainly influenced by the wavelength of the laser radiation (Fig. 5 a, b).

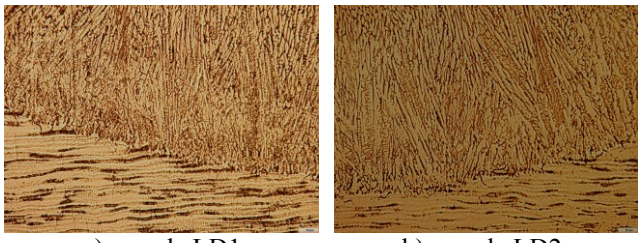

a) sample LD1 b) sample LD2

Fig. 5- Microstructure characterisation

In sample LD2 base material reached a higher temperature after performing the welding, as confirmed by the partial disappearance of the plastic deformation tensions in the material (shear bends), without affecting the structure (grain size and roundness). Also, in the case of sample LD2, as a result of the same thermal effect, the columnar structure is coarser and at the same time with more pronounced deviations from the direction of the solidification front (directional freezing). One can also notice a slight tendency towards dendritic structures, more pronounced in sample LD1, where the solidification speed was higher.

By comparing the structures resulting from welding with the two laser units mentioned (Nd:YAG and Laser Diode), which preserved almost "equal" input parameters, the following aspects become apparent (Fig. 6):

- grain size is uniform in sample LD3 and relatively uniform in sample Nd3, in which case it is also coarser;
- in sample Nd3 a tendency towards textured grain growth, according to the solidification direction, is noticed;
- the embedding state, as well as the lack of pores, are very good aspects, as there are no such defects in the structure;
- the lack of twins in austenitic grains, following solidification, confirms a characteristic pattern of solidification, for such steel type; the absence of shear

bends and lattice in austenitic grains comes to confirm a specific, cast-like stainless steel structure (AISI 316L);
- in terms of technical strength, sample LD3 will present higher properties as compared to sample Nd3 (see micro-hardness analysis).

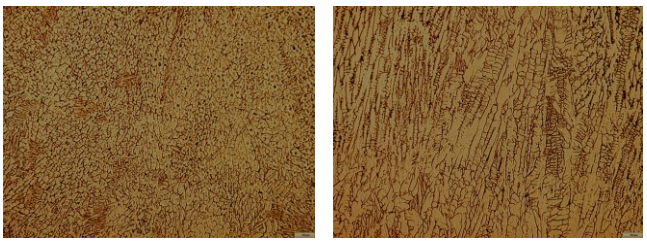

a) sample LD3 b) sample Nd3

Fig. 6- Microstructure analys resulting from welding with the two laser units mentioned (Nd:YAG and Laser Diode)

3.3 Microhardness analysis

For a complete experimental characterization of the transformations occurring in the molten material and in the heat-affected zone as a result of laser welding in case of austenitic steel AISI 316L, the analysis of the microhardness of the respective area was performed.

Hardness tests were conducted in a cross section of the weld using a pressing force of 65gf with an effective duration between 10-15 seconds. Microhardness monitoring was conducted in two directions: in the first stage- longitudinally, parallelly to the plate surface (Fig. 7) and in the second stage in a transverse direction, perpendicular to the plate surface (Fig. 8).

In Fig. 7 the hardness of the molten material is shown on a line parallel to the plate surface, at a distance of 0.5 mm from the surface and it can be seen that, from the centre of the welded zone towards the fusion limit between the molten material and the solid-state material, hardness displays a slight increase followed by a sharp increase in the limit fusion area.

Fig. 7 shows that the hardness of the molten material in the median area, close to the plate surface up to the limit area between the molten material and the solid-state material, has a value close to that of the base material. In the limit area between the molten material and solid-state material, hardness displays an exponential growth due to the high cooling rate [15]. After these elevated values, hardness shows a downward trend towards the heat-affected zone.

Increased hardness in the limit area between the molten material and solid-state material can be attributed to the increased cooling rate and the presence of unmelted grains that can become precipitation nuclei during the solidification stage [16].

In Fig. 7 and 8 one can see a notable difference between the hardness of the base material and that of the material at the boundary between the molten material and the solid-state material. That difference can be diminished by increasing the initial temperature of the base material, therefore by decreasing the temperature gradient. By increasing the initial temperature of the base material from 80°C to 120°C, a diminution of material hardness was achieved, in the limit fusion area, of about 12% for the LD generator and 5% for Nd:YAG, as measured by Hanneman microhardness testing system (Epitip, Carl Zeiss, Jena).

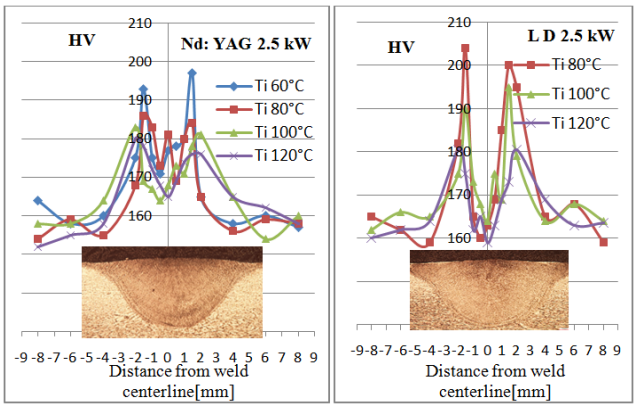

Fig. 7. Longitudinally microhardness analysis by Hanneman microhardness testing system

Depending on the wavelength, for the same input parameters, i.e. P=2.5kW, speed 10mm/s, d=3mm, Ti=80° C, a value of material hardness was achieved that was 7.5% higher when using a diode laser than in the case of using the laser unit Nd:YAG. This difference tends to disappear depending on the initial temperature of the material, decreasing for a Ti=120°C to only 1% (Fig. 8, 9).

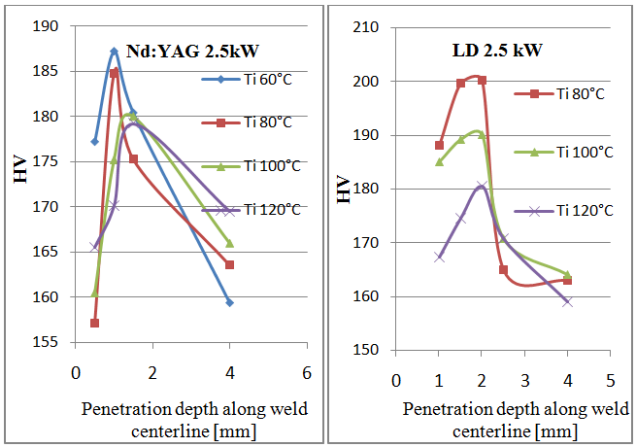

Fig. 8.Transversal microhardness analysis by Hanneman microhardness testing system

In the case of the laser welding of austenitic steels, given the very high cooling rate which influences the precipitation hardening effect [17], residual stress and microstructure, the hardness value of the material at the boundary between the molten material and the solid-state material is much higher than that of the base material. This area is the sensitive area in the case of joining by laser, the crack-generating centres being found mainly in this area. By reducing the temperature gradient between the base material and the molten material, these unwanted effects can be ameliorated.

4. Conclusions

The following conclusions have been drawn from the study of laser welding AISI316L austenitic stainless steel. The laser power input has a specific nonlinear influence on the absorptivity of material for each laser radiation wavelength. In case of CO_2 laser unit, for the welding parameters selected (laser spot diameter-3mm, speed-10mm/s), by increasing the power from 2kW to 2.5kW, the weld bead geometry undergoes minimal changes, meaning energy losses. In contrast, in case of Laser Diode unit, the weld bead geometry undergoes significant changes for the same input parameters. These issues are particularly important, allowing appropriate choice of laser generator depending on the application.

In case of laser welding, by increasing the initial temperature of the base material around 140°C a partial disappearance of the plastic deformation tensions in the material (shear bends), without affecting the structure (grain size and roundness) was registered. Besides this, a hardness reduction of the material from the limit between molten material and solid phase material by approximately 13% was obtained. This effect is accompanied by a reduction of internal tensions and of centers generating cracks and pore.

Laser welding is a complex process and through preheating the material, the geometry, microstructure and physical properties of weld bead are modified. The results of this work represent the introduction on a project in which will be developed an induction heating equipment for assisting laser welding process. Through a strict control of material temperature pre and post laser welding, a homogeneous weld bead, with low internal stress and specific physical properties can be obtained. The purpose of this technique is the avoidance of post laser welding stress relieving heat treatments that are required in case of equipment working at high pressure and high temperature variations.

Acknowledgement

The work has been funded by the Sectoral Operational Programme Human Resources Development 2007-2013 of the Ministry of European Funds through the Financial Agreement POSDRU/159/1.5/S/132395.

References

[1] Danial Kianersi , Amir Mostafaei , Ahmad Ali Amadeh, Materials and Design 61, 251 (2014).
[2] V. Geanta, I. Voiculescu, R. Ştefanoiu, D. Savastru, I. Csaki, D. Patroi, L. Leonat Optoelectron. Adv. Mater. - Rapid Comm. **7**(11-12), 874 (2013).
[3] V. Geanta, M. Taca, D.D. Daisa, I. Voiculescu, R. Ştefanescu, D.M. Constantinescu, D. Savastru, J. Optoelectron. Adv. Mater. 17(7-8), 1004 (2015);
[4] M. Sohaciu, C. Predescu, E. Vasile, E. Matei, D. Savastru, A. Berbecaru Digest Journal of Nanomaterials and Biostructures, 8(1), 367 (2013);
[5] I. B.Roman, M. H. Tierean, J. L. Ocaña, J. Optoelectron. Adv. Mater. 15(1- 2), 121 (2013).
[6] C. Predescu, N. Ghiban, M. Sohaciu, D. Savastru, E. Matei, A. Predescu, A. Berbecaru, G. Coman, Optoelectron. Adv. Mater. - Rapid Comm., **8**(1-2), 149 (2014);
[7] L. H. Hu, J. Huang , Z.G. Li, Y.X. Wu, Materials and Design **32,** 1931 (2011);
[8] I. F., Avarvarei, O., Dontu, O Turcan., R. R. Ciobanu, Device and process for increasing laser radiation absorbtivity by heating the piece to be processed in micro-production laser installations, Patent Number(s): RO129352-A2;
[9] M I Rusu, R. Zamfir, E. Ristici, D. Savastru, C. Talianu, S. Zamfir, A. Molagic, C. Cotrut J. Optoelectron. Adv. Mater., 8(1), 230 (2006),
[10] Dieter Schuocker, Handbook of the EuroLaser Academy: Volume 2, 1998; [11] William M. Steen, Laser Material Processing, Springer Verlag London, 1999;
[12] K.Suresh Kumar, Procedia Materials Science **6**, 821 (2014);
[13] Mikhail Sokolova, Antti Salminena, Physics Procedia 56, 450 (2014).
[14] I. B. Roman, M. H. Tierean, J. L. Ocaña, C. Munteanu, J. Optoelectron. Adv. Mater. **15**(7- 8), 645 (2013).
[15] V. Geanta, I. Voiculescu, R. Ştefanoiu, D. Savastru, D. Daisa J. Optoelectron. Adv. Mater. **15**(11-12), 1457 (2013);
[16] L. Zhang, J.Z.Lu, K.Y.Luo, A.X.Feng, F. Z.Dai, J.S.Zhong, M.Luo, Y.K.Zhang- Materials Science & Engineering A **561**, 136–144;
[17] O.Turcan, O.Dontu, J.L.Ocana Moreno, I.Voiculescu, D. Savastru, I.M.Vasile, J. Optoelectron. Adv. Mater., **16**(1-2), 20 (2014).

*Corresponding author: mihai.branzei@upb.ro